Energy landscape in 3D finite dust clusters derived from shell transitions

2008 J. Phys.: Condens. Matter 20 404204

(http://iopscience.iop.org/0953-8984/20/40/404204)

J. Phys.: Condens. Matter **20** (2008) 404204 (6pp) doi:10.1088/0953-8984/20/40/404204

Energy landscape in 3D finite dust clusters derived from shell transitions

A Melzer[1], S Käding[1], D Block[2] and A Piel[2]

[1] Institut für Physik, Ernst-Moritz-Arndt-Universität, D-17487 Greifswald, Germany
[2] IEAP, Christian-Albrechts-Universität, D-24098 Kiel, Germany

Received 1 April 2008, in final form 27 May 2008
Published 10 September 2008
Online at stacks.iop.org/JPhysCM/20/404204

Abstract
Experiments on three-dimensional (3D) spherical arrangements of charged dust particles in a plasma confinement (Yukawa balls) are presented. The plasma trap provides a 3D isotropic harmonic confinement in which a small number of dust particles, $N < 100$, are trapped. The particle arrangement is recorded using stereoscopic imaging. Transitions between different configurations of Yukawa balls are observed that allow us to determine the energy landscape in such a finite cluster. The experiments have been compared to molecular dynamics (MD) simulations with very good agreement.

(Some figures in this article are in colour only in the electronic version)

1. Introduction

Complex (dusty) plasmas are ideal systems for studying strongly coupled charged-particle systems. Besides electrons, ions and neutrals, a complex plasma consists of microparticles ('dust') that are charged by the continuous inflow of the plasma electrons and ions. Due to the higher electron mobility the dust particles acquire a high negative charge, leading to an electrostatic repulsion between the microparticles which is usually only moderately shielded by the ambient plasma.

The phase state of charged-particle systems is defined by two dimensionless parameters: the coupling constant Γ and the screening strength κ. When the coupling parameter $\Gamma = Z^2e^2/4\pi\epsilon_0 bkT$ exceeds the critical value ($\Gamma_{\rm crit}$ is of the order of 200 for infinite systems with pure Coulomb interaction [1]) the system is in an ordered state. Here, Z is the charge number of the microparticles, b is the interparticle spacing and T is the temperature of the microparticles. The coupling constant Γ describes the electrostatic energy of neighboring particles in units of their thermal energy. The influence of shielding of the dust charge by the ambient plasma is described by the screening strength $\kappa = b/\lambda$, where λ is the shielding length. Pure (unshielded) Coulomb interaction is retrieved for $\kappa = 0$; in dusty plasma experiments often $\kappa \approx 1$ is obtained.

Finite systems of charged particles have been investigated since Thomson's model of the atom in 1904 [2]. Three-dimensional (3D) systems of trapped charged particles that interact via (screened) electrostatic repulsion have been analyzed thoroughly in simulations; see e.g. [3–6]. Such systems, like the Yukawa balls investigated here, show a structure of nested concentric shells. The structure is usually denoted by $(N_1, N_2, \ldots)$, where N_1 is the number of particles on the inner shell, N_2 that of the second shell, etc. Experimentally, charged-particle clusters are found, e.g. as ion clusters in ion traps at low temperatures ($Z = 1$, $b \approx 10$ μm, $T = 10$ mK) that interact by a pure Coulomb potential [7] or as Yukawa balls.

Recently, it has become possible to generate three-dimensional spherical clusters of microparticles with a few to a few thousand particles trapped in a plasma environment [8]. These Yukawa balls with their highly charged microparticles ($Z \simeq 2000$) form ordered structures in a plasma environment even at room temperature and an interparticle separation of $b \approx 0.5$ mm (this corresponds to $\Gamma \simeq 500$). The Yukawa balls allow a direct observation and tracking of all trapped particles with high temporal and spatial resolution by 3D video microscopy [9, 10].

An enhanced stability of trapped charged-particle systems is found for highly symmetric configurations; the so-called magic number configurations [3, 5, 6]. Similar magic number configurations are also known for cold noble gases that form clusters with icosahedral shell structure [11, 12] or for alkali-metal, noble-metal or Si clusters [12, 13]. This suggests that geometric constraints determine the structure of different types of clusters to a large extent, although the type of bonding (van der Waals, ionic, covalent, or metallic) also influences the structure of these clusters [12].

In trapped charged-particle systems the ground state of lowest energy is often accompanied by a spectrum of metastable states with only slightly higher energy. The

metastable states are usually separated from the ground states by small energy barriers so that even at finite temperatures the charged cluster may reside in a metastable state.

As an example of the dynamical processes that can occur in charged-particle clusters, here transitions of single particles between the different shells of a Yukawa ball are investigated. The analysis of such shell transitions allows us to derive a detailed understanding of the cluster energies in the ground and metastable states. The basis for such investigations is the ability to record the 3D particle trajectories with high accuracy.

2. Finite dust clusters

In a plasma, the dust particles are subject to a number of forces. For the microspheres typically used in studies on fundamental properties of dusty plasmas, the two dominant forces are gravity and the electric field force. Also, the thermophoretic force due to temperature gradients in the neutral gas background that drives the particles towards colder regions is often applied in dusty plasmas. By tailoring these forces in combination with (dielectric) walls and electrostatic barriers, finite dust clusters can be trapped in various confinement geometries.

The total energy of N dust particles confined in a trapping potential V is given by

$$E = V(x, y, z) + \frac{Z^2 e^2}{4\pi\epsilon_0} \sum_{i>j}^{N} \frac{\exp(-r_{ij}/\lambda_D)}{r_{ij}}. \qquad (1)$$

Often, the trapping potential can be described as harmonic in every direction, resulting in

$$V(x, y, z) = \tfrac{1}{2} m(\omega_x^2 x^2 + \omega_y^2 y^2 + \omega_z^2 z^2),$$

where x, y are Cartesian coordinates in the horizontal plane and z denotes the vertical direction. The second term in the energy equation is the (screened) electrostatic energy between the particles. It is characterized by the particle charge Z and the Debye screening length λ_D. The interparticle distance between particle i and j is denoted by r_{ij}.

Experimentally, linear, one-dimensional (1D) systems have been generated by placing a narrow rectangular barrier on the electrode [14, 15] or by a groove in the electrode; see e.g. [16, 17]. This provides a confinement that is characterized by $\omega_x \ll \omega_y, \omega_z$ and thus allows a particle arrangement only along the x-direction. In these systems, wave propagation, structural transitions and the phonon spectrum have been studied [14–17].

Clusters have also been generated in two dimensions (2D); see e.g. [18–21]. There, as an example, a shallow circular parabolic depression has been manufactured into the electrode. This depression distorts the equipotential lines in the sheath and provides a radial (horizontal) confinement of the dust (i.e. $\omega_x = \omega_y \ll \omega_z$). The strong vertical confinement is due to the balance of the electric field force and gravity in the space charge sheath of the plasma where the particles are trapped. These 2D finite systems have been studied for example with respect to their structure, rotational stability and normal modes [18–21].

Recently, ball-shaped 3D clusters (so-called Yukawa balls) have been generated successfully in the laboratory [8, 22]. These Yukawa balls are confined in a specially designed trap (see below) where the dominant action of gravity is (partially) compensated by an upward thermophoretic force. Careful adjustment of the plasma parameters allows us to form a spherical trap with $\omega_x = \omega_y = \omega_z \equiv \omega_0$. The trapped particles form a compact convex structure with concentric 'onion' shells [8]. Yukawa balls have been studied in view of their structural properties [8, 23, 24] as well as with respect to shell transitions [25]. Here, a specific cluster configuration is analyzed to investigate the energy landscape of finite clusters during a self-excited transition between different configurations.

3. Experimental setup

The investigation of structural and dynamical properties of 3D particle systems requires the simultaneous measurement of all particle coordinates. Here, a three-camera stereoscopic setup is used where the cameras are oriented pairwise perpendicular to each other to keep the observation geometry as simple as possible (see figure 1). The cameras have a spatial resolution of 1280×1024 pixels. The three cameras are synchronized by an external trigger signal and are run with a frame rate of up to 50 fps (frames per second) in our experiments.

The observable volume is limited by the focal depth to about $10 \times 10 \times 10$ mm^3. An expanded laser beam (Nd:YAG at a wavelength of 532 nm and an output power of 600 mW) illuminates all the particles in this volume. The dust cloud is illuminated from two directions so that the horizontal cameras observe the particles in forward scattered light, which offers a higher light intensity and, in turn, an increased focal depth due to possible smaller camera apertures.

The experiments have been performed in a capacitively-coupled asymmetric rf discharge at 13.56 MHz in argon at a gas pressure of 90 Pa and a discharge power between 2 and 7.5 W. The particle confinement follows the technique of Arp *et al* [8]: commercially available monodisperse plastic spheres of 3.46 μm diameter (mass $m = 3.28 \times 10^{-14}$ kg) with a size variance of 2% are dropped into the discharge. The particles are confined horizontally by a cubic glass cuvette placed on the lower electrode. Vertically, gravity is compensated by the combined action of an upward thermophoretic force due to heating of the lower electrode and a weak electric field near the sheath edge of the lower electrode [26]. Thus, the particles are trapped in a weak plasma inside the glass box near the sheath boundaries to the lower electrode and the glass walls. In this trap, Yukawa balls are produced where the particles arrange in a spherical cloud with nested concentric shells.

To recover the 3D positions of all particles with high spatial and temporal resolution, first the 2D coordinates of the particles in each camera are determined. An example of typical raw images is also shown in figure 1. Then, corresponding particles are identified in the images of the front-view, side-view and top-view camera. The search for correspondences is simplified by the orthogonal geometry of the cameras, which decreases the number of eligible candidates. Having

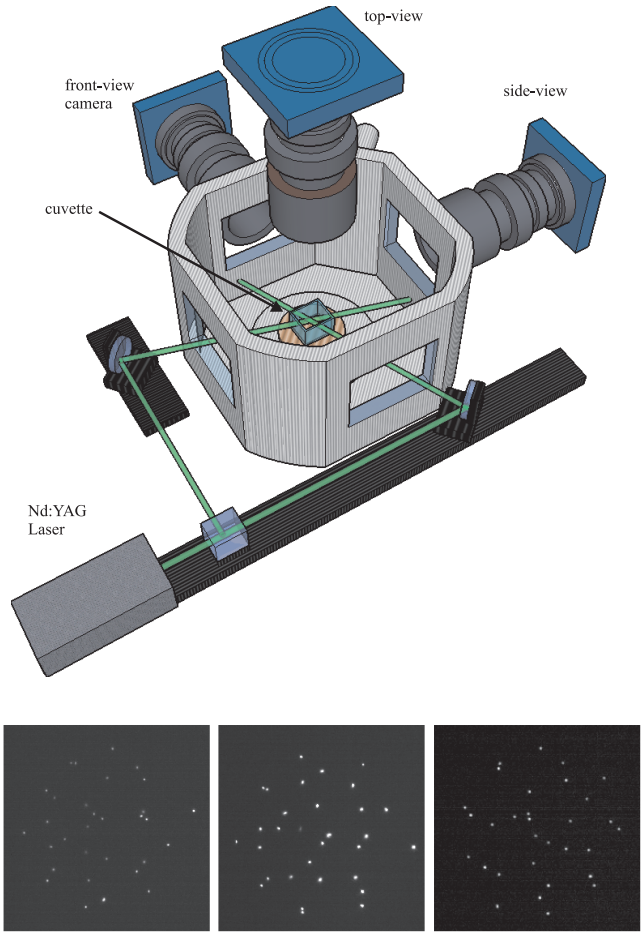

Figure 1. Scheme of the stereoscopic camera setup and illumination. Three pairwise perpendicular video cameras observe the Yukawa ball inside the glass cuvette. The dust particles are illuminated by an expanded laser beam from two directions. The observation of the particles in forward scattered light by the horizontal cameras ensures a higher focal depth. The lower panels show the raw video still images of a Yukawa ball with $N = 31$ particles recorded by the three cameras. The main advantage is that all particles are seen in at least two cameras.

identified corresponding particles, their 3D positions are easily determined. Finally, the particle trajectories are determined by following each particle from one frame to the next. A detailed description of the data analysis is given in [25].

4. Experimental results

Since our aim is to investigate the energy landscape of confined particle clusters by exploiting self-excited transitions between different cluster configurations, we briefly describe their structural properties. Our investigations of the structure cover almost the full range of particle numbers ($1 < N < 100$ [25]). In the description here, we concentrate on clusters with $N = 31$, 52 and 91 particles. For the analysis of the energy landscape we focus on the $N = 31$ cluster.

4.1. Structure of Yukawa balls

From previous experiments [8, 27] and simulations [3, 5, 23, 28, 29] it is known that finite systems of dust particles trapped in a spherical confinement arrange in nested spherical shells with occupation numbers $(N_1, N_2, \ldots)$.

Snap shots of observed configurations of Yukawa balls of different particle number are shown in figure 2. It is seen that the Yukawa balls indeed arrange in concentric shells. The $N = 31$ cluster shown here has a configuration (5, 26) where 5 particles are on the inner shell and 26 are on the outer. The $N = 52$ cluster has three shells with a configuration (1, 11, 40). Finally, the $N = 91$ cluster has a three-shell configuration with (4, 25, 62). In each case, the interparticle distance is about $b = 500\ \mu$m.

In this respect, it is interesting to note that the ground-state configuration for the $N = 31$ cluster is (4, 27) for pure Coulomb interaction. For screened interaction, a higher occupation on the inner shells on the expense of the outer is expected [23]. However, for all experimentally accessible values of the screening strength $\kappa = b/\lambda_D < 1.5$ the ground state remains (4, 27). Thus, the observed configuration (5, 26) is a metastable state. Such a preference of metastable configurations is not unlikely [24, 25].

Similarly, the (1, 11, 40) configuration of the $N = 52$ cluster is a metastable state. Ground-state configurations, as determined from simulations, are (10, 42), (12, 40) and (1, 12, 39) for increasing screening strength κ. Thus, also, for $N = 52$ a ground-state configuration is found in the experiment. Finally, for $N = 91$ the ground state for pure Coulomb interaction is (3, 22, 66). Here, in the experiment, with the configuration (4, 25, 62) we again find a higher occupation of the inner shells compared to the pure Coulomb case.

In conclusion, in the analysis of the structure of Yukawa balls, metastable states are frequently found.

4.2. Energy landscape and shell transitions

We now like to address the question of transitions between different states and the underlying energy landscape. Here, specifically, a shell transition of the cluster with $N = 31$ will be analyzed in more detail with respect to the energies involved. The search for transitions between configurations starts with the observation of the cluster for several minutes. Figure 3 shows the trajectories of all particles over 100 s in cylindrical coordinates $\rho = \sqrt{x^2 + y^2}$ and z. A shell transition with a change of the configuration is easily recognized. A particle from the outer shell moves towards the inner, resulting in a change of configurations from (4, 27) to (5, 26). Thus, here, a transition from the ground state to the metastable state is observed. This transition is driven by only the thermal energy of the cluster. No other forces have been applied.

We now analyze this transition in more detail. In figure 4(a) the radial position ($r = \sqrt{x^2 + y^2 + z^2}$) of the traveling particle is shown as a function of time. In the beginning of the sequence, the cluster is in a (4, 27) configuration. The traveling particle first stays in the outer shell (at a radial position around $r \approx 0.64$ mm) and only performs thermal Brownian fluctuations around its equilibrium position. However, after $t = 430$ s the particle starts to leave the outer shell. The particle moves inwards and reaches the innermost position ($r = 0.34$ mm) at about $t = 517$ s, where

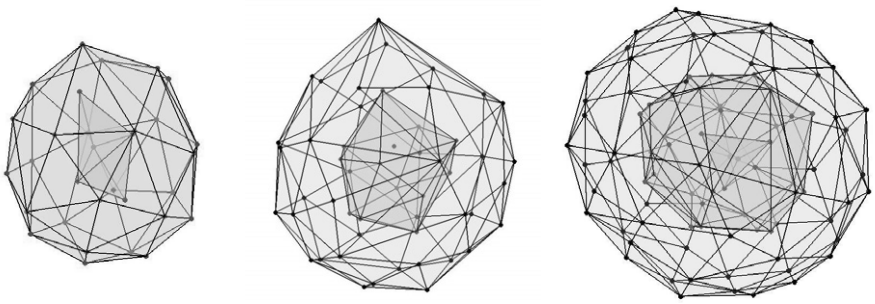

Figure 2. Cluster configurations reconstructed from single video snap shots with $N = 31$, 52, and 91. The Yukawa balls consist of concentric shells with the configurations (5, 26) for the $N = 31$ cluster, (1, 11, 40) for the $N = 52$ cluster, and (4, 25, 62) for the $N = 91$ cluster.

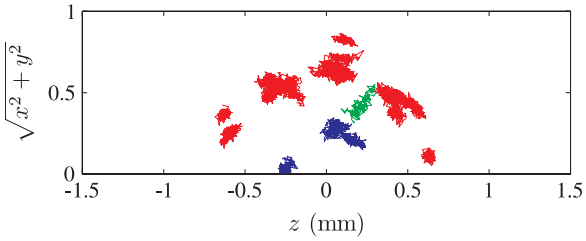

Figure 3. Particle trajectories in cylindrical coordinates of a cluster with $N = 31$. The configuration changes from (4, 27) to (5, 26).

it resides for a short moment before it slowly returns to the outer shell. During this transition the radial positions of the other 30 particles stayed nearly constant. This transition is obviously a very slow, gradual process. It is decisively different from the hopping motion observed in 2D crystals occurring on the timescale of the Einstein frequency of nearest-neighbor oscillations (typically of the order of a few Hertz [30]).

Obviously, a transition from the ground state (4, 27) to the metastable state is energetically unfavorable. To quantify this energy cost, we have modeled this transition. For that purpose, a molecular dynamics (MD) simulation of an $N = 31$ particle cluster is performed in real physical units, since a quantitative comparison with the experiment is intended. To assure a crystalline state of the cluster, a dust charge of $Z = 2000$ is required. This charge value is in agreement with previous investigations [23, 26]. In addition, the screening parameter was taken as $\kappa \approx 1$, as suggested by previous investigations [23, 26]. Finally, the confinement strength of the 3D isotropic parabolic trapping potential is chosen to match the experimental cluster size in the simulations as $\omega_0 \approx 40\ \mathrm{s}^{-1}$. This agrees with values obtained in previous experiments using independent methods [26] and accounting for the slightly different plasma conditions compared to [26]. In the MD simulation, a particle from the outer shell is then deliberately moved to the inner shell and the corresponding energy, according to equation (1), is calculated.

The simulated energy landscape for the transition from (4, 27) to (5, 26) thus calculated is shown in figure 4(b). The ground and metastable states differ in energy by $E/N = 24$ meV. However, to reach the metastable state, a slightly higher energy barrier of $E/N = 26$ meV (for the more favorable scenario 1) has to be overcome. These numbers indicate that the metastable state should be energetically accessible at room temperature. It can be assumed reasonably that the kinetic temperature of the dust particles in the cluster is room temperature, due to the strong friction with the neutral gas background.

The transition (4, 27) to (5, 26) can occur in two scenarios that are illustrated in figure 5. In the ground-state configuration the four particles on the inner shell form a tetrahedron, as expected. The traveling particle can then arrive towards one of the faces of the tetrahedron (scenario 1, figure 5(a)) or towards one of the edges (scenario 2, figure 5(b)). In both cases a double tetrahedron configuration of the five inner-shell particles is formed. Scenario 2, however, requires that the previous edge particle is displaced to the tip of the double tetrahedron. This requires additional energy, which is seen as the additional hump in the energy landscape near $r = 0.35$ mm. Further, it is interesting to note that the minimum energy of the metastable state appears at different radial positions. This is due to the fact that in scenario 1 the approaching particle forms the tip of the newly formed double tetrahedron, whereas in scenario 2 it becomes one of the particles in the central triangle. Since the tip has a larger distance from the center than the triangle particle, equilibrium is found at two different radial positions. Scenario 1 is found for a slow equilibrium transition; scenario 2 can be realized when the transition is faster. Then the inner tetrahedron has no time to rotate in such a way that the traveling particle approaches the face of the tetrahedron. For the timescale of the observed transition, both scenarios occur in the simulation.

From the observed trajectory, however, it is seen that the first scenario is realized in the experiment, since the traveling approaches the larger radial equilibrium at the tip of the inner double tetrahedron.

To illustrate the capability of the experimental diagnostics, the energy landscape is estimated from the trajectory of the traveling particle. Therefore, the friction energy that dissipated by the traveling particle is analyzed. The friction energy is derived from

$$\mathrm{d}E = m\beta\dot{r}\,\mathrm{d}r, \tag{2}$$

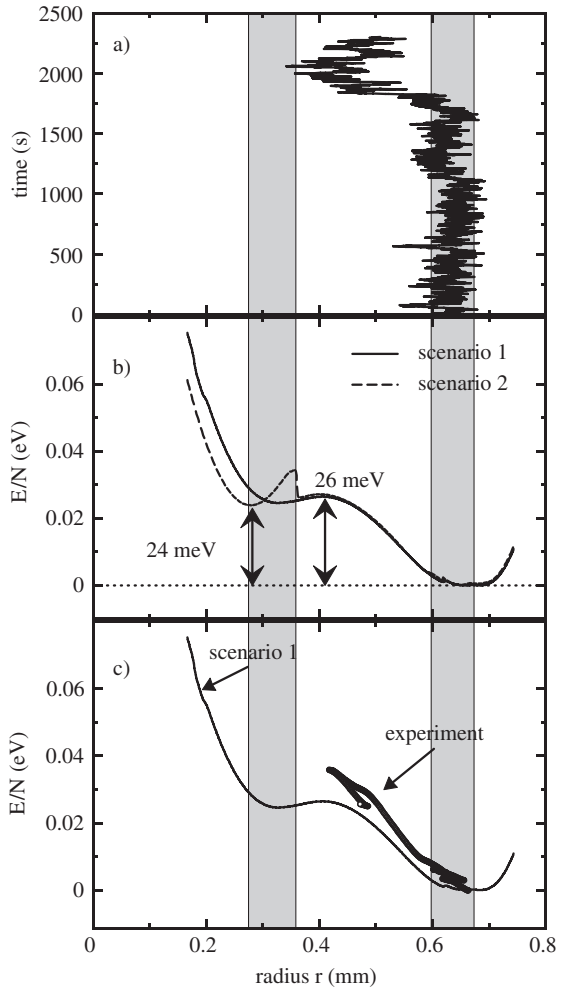

Figure 4. (a) Radial position ($r = \sqrt{x^2 + y^2 + z^2}$) of the traveling particle as a function of time, causing a configuration change from (4, 27) to (5, 26). The gray vertical bars indicate the radial positions of the inner and outer shells of the $N = 31$ cluster, respectively. (b) Energy landscape of the $N = 31$ particle cluster. Here, the energy per particle, E/N, derived from simulation is shown for a particle traveling from the outer shell inwards. Here, two scenarios are possible, which are indicated in figure 5. To reach the (5, 26) configuration starting from (4, 27), an energy barrier has to be overcome. (c) Comparison of the energy derived from the frictional trajectory of the traveling particle with the energy landscape of (b).

where the Epstein friction coefficient is $\beta = 210\ \mathrm{s}^{-1}$ for a gas pressure of 90 Pa [31] and the particle mass is $m = 3.3 \times 10^{-14}$ kg. Here, dE is the change in friction energy when the particle is moved by a radial distance dr against friction. Inertia can be neglected due to the slow gradual process, and other forces have not been applied. Here, this friction energy is calculated from the experiment when the particle travels from the outer shell to the inner shell. The energy thus derived is plotted against the simulated energy for the transition in figure 4(c). The experimentally determined friction energy follows the simulated energy quite nicely. This indicated that indeed the energy landscape can be deduced from the analysis of the particle motion in a cluster.

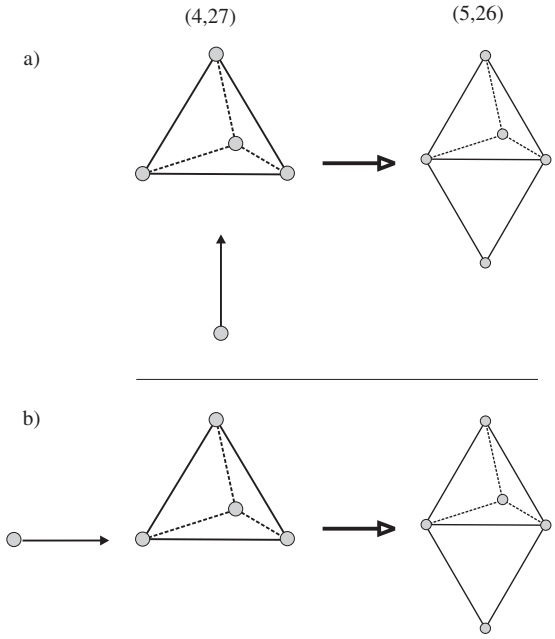

Figure 5. Illustration of scenario 1 (a) and scenario 2 (b) when the traveling particle approaches the inner shell. See text for details.

5. Summary

In conclusion, we have presented experiments on the energies between different configurations of 3D spherical Yukawa balls. Here, the stereoscopic diagnostic of the Yukawa balls allows a deep and detailed analysis of the 3D particle positions and motions.

From long-run experiments, self-excited transitions between different (metastable) configurations of small Yukawa balls are observed. These clusters often show metastable configurations rather than ground states.

From the analysis of a transition in a specific cluster, the energy has been derived from the frictional energy of the traveling particle. The derived energy has been found to be in very good agreement with the energy landscape determined from MD simulations.

Acknowledgments

We thank M Bonitz and H Baumgartner for fruitful discussions. Financial support from the Deutsche Forschungsgemeinschaft via SFB-TR24 grants A2 and A3 is gratefully acknowledged.

References

[1] Ichimaru S 1986 *Plasma Physics: An Introduction to Statistical Physics of Charged Particles* (Menlo Park, CA: Benjamin/Cummings)
[2] Thomson J J 1904 *Phil. Mag.* **39** 237
[3] Hasse R W and Avilov V V 1991 *Phys. Rev.* A **44** 4506
[4] Dubin D H E and O'Neill T M 1999 *Rev. Mod. Phys.* **71** 87
[5] Apolinario S, Partoens B and Peters F 2007 *New J. Phys.* **9** 283
[6] Ludwig P, Kosse S and Bonitz M 2005 *Phys. Rev.* E **71** 046403

[7] Mortensen A, Nielsen E, Matthey T and Drewsen M 2006 *Phys. Rev. Lett.* **96** 103001
[8] Arp O, Block D, Piel A and Melzer A 2004 *Phys. Rev. Lett.* **93** 165004
[9] Käding S and Melzer A 2006 *Phys. Plasmas* **13** 090701
[10] Antonova T, Annaratone B M, Goldbeck D D, Yaroshenko V, Thomas H M and Morfill G E 2006 *Phys. Rev. Lett.* **96** 115001
[11] Mackay A 1962 *Acta Crystallogr.* **15** 916
[12] Baletto F and Ferrando R 2005 *Rev. Mod. Phys.* **77** 371
[13] Kostko O, Huber B, Moseler M and von Issendorff B 2007 *Phys. Rev. Lett.* **98** 043401
[14] Homann A, Melzer A, Peters S, Madani R and Piel A 1997 *Phys. Rev.* E **56** 7138
[15] Melzer A 2006 *Phys. Rev.* E **73** 056404
[16] Liu B, Avinash K and Goree J 2003 *Phys. Rev. Lett.* **91** 255003
[17] Liu B and Goree J 2005 *Phys. Rev.* E **71** 046410
[18] Juan W-T, Huang Z-H, Hsu J-W, Lai Y-J and L I 1998 *Phys. Rev.* E **58** 6947
[19] Klindworth M, Melzer A, Piel A and Schweigert V 2000 *Phys. Rev.* B **61** 8404
[20] Melzer A 2003 *Phys. Rev.* E **67** 016411
[21] Sheridan T E 2005 *Phys. Rev.* E **72** 026405
[22] Antonova T, Annaratone B M, Goldbeck D D, Yaroshenko V, Thomas H M and Morfill G E 2005 *AIP Conf. Proc.* **799** 299
[23] Bonitz M, Block D, Arp O, Golubnychiy V, Baumgartner H, Ludwig P, Piel A and Filinov A 2006 *Phys. Rev. Lett.* **96** 075001
[24] Block D, Käding S, Melzer A, Piel A, Baumgartner H and Bonitz M 2008 *Phys. Plasmas* **15** 040701
[25] Käding S, Block D, Melzer A, Piel A, Kählert H, Ludwig P and Bonitz M 2008 *Phys. Plasmas* submitted
[26] Arp O, Block D, Klindworth M and Piel A 2005 *Phys. Plasmas* **12** 122102
[27] Block D *et al* 2007 *Plasma Phys. Control. Fusion* **49** B109
[28] Totsuji H, Ogawa T, Totsuji C and Tsuruta K 2005 *Phys. Rev.* E **72** 036406
[29] Baumgartner H, Kählert H, Golobnychiy V, Henning C, Käding S, Melzer A and Bonitz M 2007 *Contrib. Plasma Phys.* **47** 281
[30] Chan C-L, Woon W Y and L I 2004 *Phys. Rev. Lett.* **93** 220602
[31] Epstein P S 1924 *Phys. Rev.* **23** 710